J Sol-Gel Sci Technol (2009) 51:204–214
DOI 10.1007/s10971-009-1972-8

ORIGINAL PAPER

Synthesis of Ag and Ag/SiO_2 sols by solvothermal method and their bactericidal activity

B. Mahltig · E. Gutmann · M. Reibold · D. C. Meyer · H. Böttcher

Received: 19 December 2008 / Accepted: 2 April 2009 / Published online: 21 April 2009

Abstract Ag and Ag/SiO_2 sols containing nanocrystalline silver particles can be advantageously prepared by solvothermal methods using an autoclave with conventional thermal or microwave heating. In this process, the reduction of silver salts can be realized with alcohols like ethanol in the presence of polyvinylpyrrolidone at temperatures of more than 120 °C. Furthermore a combination of silver salt reduction with hydrolysis of alkoxysilanes during the solvothermal process can yield Ag/SiO_2 composite sols. Particle size and crystallinity of as-prepared particles are analyzed by means of X-ray diffraction and high-resolution transmission electron microscopy. Nanosized silver particles gained by this process exhibit antimicrobial properties that are investigated in detail after application on textile fabrics.

Keywords Solvothermal · Silver · Textile · Antimicrobial

1 Introduction

The use of nanosized silver particles e.g., as antimicrobial agents or optical filters is of scientific and economic interest [1–5]. For antimicrobial applications, e.g., to prevent healthcare-associated infections, employing silver particles is especially advantageous, since they exhibit a high biocide efficiency against a broad range of germs already at low concentration and only a small tendency to resistance formation [1, 6, 7]. Thus, silver containing materials are also highly advantageous for medical applications for example as silver refined textile fabrics for the treatment of atopic dermatitis or for additional skin-therapy of patients with diabetes [8].

Temperature-sensitive materials like textiles or wood can be easily equipped with antimicrobial properties by using the sol-gel technique [9–13]. This method enables the combination with other functional properties like water repellence, dyeing or UV protection [14–18]. Embedding of nanosized silver in inorganic sol-gel matrices can be used for stabilization of silver particles and to enhance its fixation to the coated substrates [19–25]. Different methods are reported for the preparation of silver particles and its application onto various substrates, e.g., the thermal decomposition of deposited $AgNO_3$ at temperatures above 300 °C [26–28]. However, these high processing temperatures are only convenient for coatings on glass or metal substrates but not for temperature-sensitive materials [9–11].

The synthesis of silver clusters under ambient conditions can be performed by precipitation of AgCl and illumination [29]. Also the combination of $AgNO_3$ with reductive agents is an appropriate method. Useful reductive agents are $NaBH_4$, ascorbic acid [30, 31] or hydrazine hydrate in combination with sodium dodecyl sulphate and citrate as stabilizing agents [32]. The combination of reductive agents and polymeric stabilizers like polyvinylpyrrolidone PVP [33–39] is especially advantageous. Hereby PVP acts as complexing agent that prevents the aggregation of silver particles in solution by coordination between silver and PVP [40].

B. Mahltig (✉) · H. Böttcher
Gesellschaft zur Förderung von Medizin-, Bio- und Umwelttechnologien e.V., GMBU e.V., Postfach 520165, 01317 Dresden, Germany
e-mail: mahltig@gmbu.de

E. Gutmann · M. Reibold · D. C. Meyer
Technische Universität Dresden, Institut für Strukturphysik, 01062 Dresden, Germany

Thus, stable coating solutions containing silver particles can be gained [33], similarly to those obtained for example by the polyol process with the solvent ethylene glycol driven at temperatures above 100 °C [5, 41–45]. Beside this function as complexing agent, PVP is also reported to act as reductive agent for $AgNO_3$ in a polymer paste during stirring at room temperature [38]. A further simple method to prepare nanosized silver particles is the reduction of $AgNO_3$ by the solvent ethanol and the stabilization of the particles formed by functionalized silane compounds. This reaction requires a thermal treatment of the solution under reflux [46, 47]. However in presence of complexing agents like PVP, due to complex formation of PVP with Ag^+, the redox potential of Ag^+ is decreased. Thereby, probably harsher reaction conditions are necessary for the reduction of Ag^+, as for example provided by higher temperatures of a solvothermal process [47].

Analogously to a reflux thermal treatment under atmospheric pressure, a solvothermal preparation of silver particles is reported for temperatures up to 200 °C under increased pressure [25, 48–53]. The nanosized silver is mostly gained as precipitate and powder. Especially emphasized should be the intensive discussion of Tian et al. [53] reporting the formation of Ag nanoparticles by reduction of $AgNO_3$ in presence of dodecanthiol in a solvothermal process. Under the conditions reported therein, $AgNO_3$ is probably reduced by ethanol at processing temperatures of ≥180 °C. At lower temperatures of 100 °C a yellow precipitate of a layered-like $AgS(CH_2)_{11}CH_3$ complex is formed. Also the impregnation of cotton with solution of $AgNO_3$ and its reduction to elemental nanoparticular silver in an autoclave system at a temperature of 120 °C is reported [54]. In this in situ synthesis, the reduction of $AgNO_3$ is probably caused by terminal aldehyde groups on the cotton fabrics.

In order to apply silver particles onto different surfaces it is, however, more convenient to have a liquid solution of stabilized silver particles which can be easily applied by dip-coating or spraying. Therefore, it could be advantageously to develop a preparation method which combines both, the solvothermal reduction in ethanol and the use of PVP as stabilizer. This approach has the advantage that no further reductive agent is required and furthermore, a combination with silica sol particles is simultaneously possible by adding the silane precursor tetraethoxysilane (TEOS). The following investigations describe the conditions of solvothermal preparation and resulting features of Ag and Ag/SiO_2 coating solutions. Furthermore, application of as-prepared coating solutions onto textiles is performed and its antimicrobial properties are tested.

2 Experimental procedures

2.1 Preparation of Ag nanoparticles and Ag/SiO_2 sols

Silver sol *A* is prepared by solvothermal treatment of a mixture of 100 mL ethanol, 1 g polyvinylpyrrolidone (PVP) (trademark: K25, $M_W \sim 24000$ g/mol, >99.9%, supplier: Carl Roth GmbH, Germany) and 1 g $AgNO_3$ (>99.9%, supplier: Carl Roth GmbH, Germany) in 3 mL of 0.01-N-HNO_3. Silver-silica sol *B* is prepared by solvothermal treatment of a mixture of 100 mL ethanol, 20 mL tetraethoxysilane TEOS (trademark: Wacker Silikat TES28, >99%, supplier: Wacker Chemie GmbH, Germany), 1 g polyvinylpyrrolidone and 1 g $AgNO_3$ in 3 mL of 0.01-N-HNO_3. The solvothermal treatment is performed in autoclaves with conventional thermal heating and by means of microwave heating. As conventional autoclave a commercially available reactor of Berghof Instruments GmbH is used (Hochdruck-Laborreaktor BR-500). This reactor contains a 500 mL teflon vessel with a mechanical stirrer. Process temperatures between 80 and 160 °C are applied for 1 h. The duration of heating-up and cooling is about 30 min and 3 h, respectively. For taking samples during the solvothermal process a commercially available reactor Büchi (Ecoclave 075, type 1) is used. This reactor contains a 500 mL glass vessel with a mechanical stirrer. The process temperatures are set at 100 and 120 °C for a time duration up to 5 h. After reaching the reaction temperature (after about 30 min) samples are taken from the reaction solution as a function of time. As microwave autoclave a commercial reactor Discover Labmate™/CEM GmbH (250 Watt) is used. This reactor contains an 80 mL glass vessel with a magnetic stirrer. The process temperatures are set in a range from 80 to 160 °C involving reaction pressures between 0.5 and 13.5 bar. This process comprises a temperature raise of 3 min up to the final reaction temperature, a reaction period of 30 min and a cooling-down to room temperature of finally 20 min. In consequence of the direct energy transfer from microwaves to the reaction solution microwave-assisted synthesis enables such a rapid heating [55, 56]. For application onto textiles, viscose fabrics are dip-coated from the prepared solution. After dipping, the samples are dried at room temperature and annealed at a temperature of 120 °C for 30 min.

2.2 Characterization of Ag nanoparticles and Ag/SiO_2 sols

The presence of crystalline silver and the mean sizes of silver crystallites are determined by means of X-ray diffraction (XRD). These investigations are performed with liquid sols, dried samples on glass substrates and dried

powder samples, which are obtained after evaporation of the solvent at room temperature after a time duration of 24 h. For liquid samples, 6 mL of the sol are filled into a cavity of an aluminum disc and covered with a polypropylene foil to prevent solvent evaporation. The XRD patterns of liquid sols are recorded using a vertical X-ray diffractometer D8 (Bruker AXS) whereas for powder samples and coatings on glass slides an X-ray diffractometer URD 6 (Seifert FPM) is applied. The diffraction patterns measured are analyzed qualitatively using the PDF-2 database [57]. The mean size of nanocrystalline silver particles is derived from a quantitative phase analysis of the diffraction patterns performed using the computer program TOPAS [58]. Hereby XRD reflection profiles are analysed using a *Fundamental Parameters Approach* convolution algorithm [59] that includes the refinement of the full-width-at-half-maximum (FWHM) of a Lorentzian profile to account for sample induced diffraction line broadening. For all refinements, a crystal structure of silver according to the Inorganic Crystal Structure Database (ICSD) [60] collection code N° 64706 [61] is applied. In advance the X-ray emission profile and instrumental parameters of the diffraction experiment have been determined by analyzing the diffraction pattern of a Silicon standard powder (NIST SRM 640c). For all fits quality parameters R_{wp} of less than 6.5% are obtained. With respect to serial correlation effects of parameters refined standard deviations of the mean crystallite size are corrected according to [62]. High-resolution transmission electron microscopy (HRTEM) is used to determine the particle size and morphology of particulate sol components. For sample preparation 200 mesh copper grids containing a graphite membrane of 20 nm thickness (Plano) are used. A drop of the sols is applied to the copper grids and afterwards dried for at least 24 h at room temperature. As-prepared samples are investigated using a Philips TECNAI F20 TEM with CS correction. For an analysis of crystallite *d*-spacings in the HRTEM images the crystal structures of silver and rhombohedral $AgNO_3$ according to ICSD collection code N° 64706 [61] and 35157 [63], respectively, are applied. The silver ion concentration in the coating solution is potentiometrically determined using a Silver/Sulfide Combination Electrode Ag/S 800 (WTW GmbH, Weilheim, Germany). The UV-vis transmission spectra of as-prepared solutions are measured using an UV-NIR spectrometer Zeiss MCS 501 UV-NIR. The particle size distribution in liquid sols is measured by Dynamic Light Scattering (DLS) with the commercially available device Zetasizer 1000H Sa/Malvern Instruments. Hereby, the sols are diluted with ethanol in a volume ratio of 1:50. The antimicrobial activity against the bacteria *Escherichia coli* of silver containing textile samples is determined as described in a previous study [22]. The wash fastness of the coated textiles is tested with a commercial washing machine according to DIN EN ISO 6330. Five washing cycles at 40 °C with an ECE washing powder (according to ISO 105-C08/C09, supplied by EMPA) are applied. After washing, the textile fabrics are dried at room temperature and their antimicrobial activity is tested.

3 Results and discussion

3.1 Solvothermal preparation of Ag nanoparticles and Ag/SiO_2 sols

In dependence on the temperature regime (without TEOS) the color of sol *A* changes from dark red (120 °C) to light brown at higher temperatures (see Fig. 1). In accordance with the color change, the Ag^+ concentration in the solution is decreased with increasing temperature of the solvothermal process (Figs. 1, 2). The comparison of different autoclave systems (conventional and microwave heating) exhibits the same tendency of a decrease of Ag^+ concentration. However, by using the microwave autoclave the decrease starts at higher temperatures which could be explained by the shorter reaction time of 30 min but also by the shorter heating and cooling time of the microwave processing regime applied. In literature it is often stated that microwave-assisted synthesis is faster and works at lower temperature than conventional heating [55, 56]. In contrast, for the Ag^+ reduction to silver nanoparticles in presence of PVP reported here, no significant acceleration of the reaction is observed with microwave heating. Under the solvothermal conditions chosen, the reduction of $AgNO_3$ to crystalline silver is probably driven by the reaction with the solvent ethanol [46, 47] which is also reported to take place even under reflux conditions at 70 °C [46]. However, the complexation of the solved Ag^+ ions by PVP decreases their redox potential [47]. For this reason, harsher solvothermal reaction conditions of temperatures above 120 °C are necessary for a reduction of $AgNO_3$. The presence of PVP in the reaction solution is necessary to stabilize the formed silver particles by complex bonding and to preserve them from aggregation [33]. For comparison, the solvothermal reduction of $AgNO_3$ is also investigated in presence of TEOS (sol *B*) which leads to the formation of SiO_2 particles by hydrolysis under the acidic conditions chosen. In presence of SiO_2, black solutions are gained by the solvothermal processes at temperatures higher than 120 °C (Fig. 1). However, a significant decrease in Ag^+ concentration is only determined at temperatures above 130 °C (Fig. 2), indicating that in presence of SiO_2 the Ag^+ reduction is delayed when compared with sol *A*. In order to gain information about the dependence of

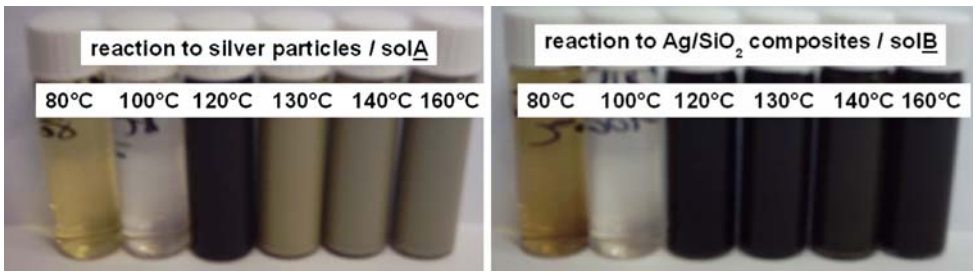

Fig. 1 Photographs of the reaction solutions gained from solvothermal processes driven at different temperatures

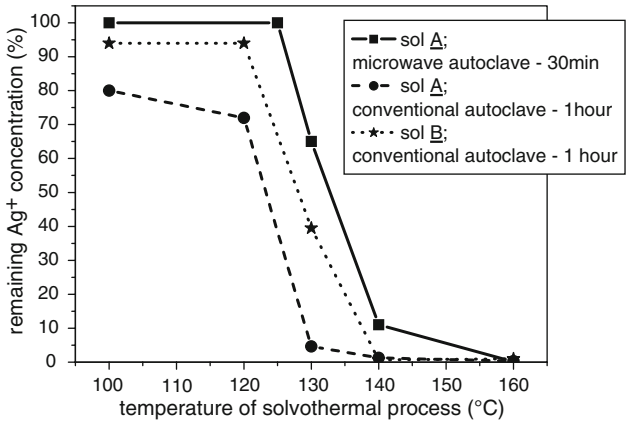

Fig. 2 Ag^+ concentration compared to a system without solvothermal treatment of the sols *A* and *B* as function of temperature of the solvothermal process

the reaction rate of silver formation on the solvothermal process duration, samples are taken directly during the solvothermal process and their Ag^+ concentration is determined. Runs are performed with sol *A* at 100 and 120 °C for a duration up to 5 h. At the process temperature of 100 °C no decrease of Ag^+ concentration was observed even after 5 h. In the first 30 min at the process temperature of 120 °C, no decrease in Ag^+ is observed which corresponds to the results gained from the microwave procedure. During longer treatment, the Ag^+ reduction starts after 1 h and finally, after 4 h less than 3% of Ag^+ remains. The rate of the silver formation in sol *B* is also investigated as a function of time at temperatures of 120 and 130 °C. At 120 °C no significant decrease of Ag^+ concentration is determined after 5 h, while at 130 °C after 1 h the Ag^+ concentration is decreased to 40% and after 5 h only a concentration of less than 1% remains. This reaction is quite fast when compared with the solvothermal reduction of AgCl in PVP/ethylene glycol solution reported in literature to happen at 160 °C after 2 h [64]. Altogether, it can be concluded that for the type of solvothermal reaction reported here it is necessary to strictly control the reaction temperature and keep it in a very small variation. Even a decrease in the reaction temperature of only 10 °C could decelerate the reaction strongly or even inhibit it completely.

3.2 Particle properties

The decrease of Ag^+ concentration in the sol *A* with increasing temperature of the solvothermal process is in good accordance with the results gained from XRD investigations of the liquid sol (Fig. 3), showing that crystalline silver (PDF Card N° 4-783) is formed at process temperatures above 120 °C. Equivalent results are gained by XRD investigations on dried materials of sol *A* (Fig. 4), displaying reflections of crystalline silver in the diffraction patterns of sols prepared at temperatures above 120 °C from which mean crystallite sizes in the range of 30–49 nm (Table 1) are obtained by quantitative analysis. Altogether the size of crystallites is not considerably influenced by the processing temperature. If the solvothermal process is driven at lower temperatures, only the remaining educt $AgNO_3$ (PDF Card N° 43-649) is determined by XRD (Fig. 4). The determined crystalline $AgNO_3$ is probably the result of recrystallisation of solved $AgNO_3$ during the sample drying for XRD measurements. Similar results are gained from XRD measurements of the dried sol *B*. When processed at the temperature of 120 °C, only the educt $AgNO_3$ can be determined, while after processing at 130 °C both $AgNO_3$ and crystalline silver are present in the same sample after 1 h duration of the process. After

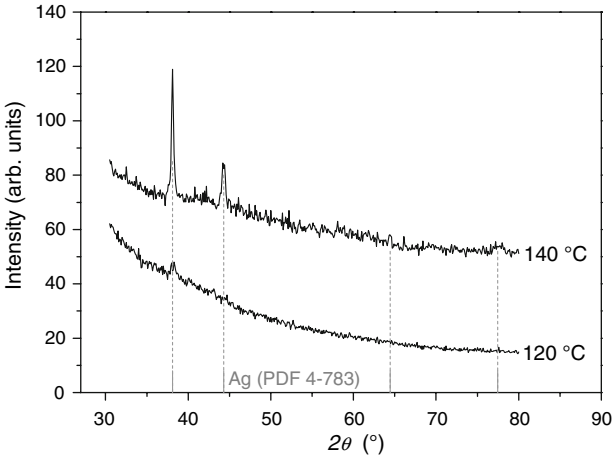

Fig. 3 XRD patterns of liquid sol *A* treated in the solvothermal process for 1 h at 120 and 140 °C, respectively

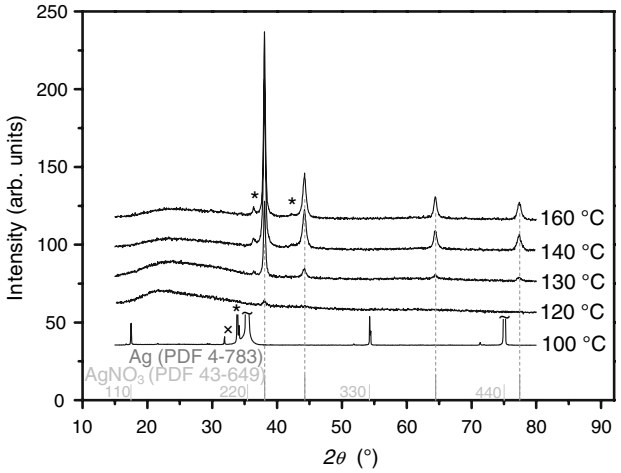

Fig. 4 XRD patterns of dried materials gained from sol *A* treated for 1 h in the conventional solvothermal process at different temperatures. Reflections marked with (*) correspond to parasitic W-Lα radiation and those marked with (*x*) to Cu-Kβ radiation present in the X-ray tube emission spectrum

Table 1 Mean crystallite size of silver nanoparticles obtained by quantitative analysis of the XRD patterns (drawn in Figs. 5, 6) of coatings on glass (sol *A*) and dried sol powders (sol *B*) prepared from coating solutions after solvothermal treatment for 1 h at the temperatures indicated

Sol	Solvothermal temperature (°C)	Mean crystallite size (nm)
Sol *A*	120	(40 ± 10)
	130	(49 ± 2)
	140	(30.4 ± 0.8)
	160	(38 ± 1)
Sol *B*	130	(16.3 ± 0.5)
	140	(18.3 ± 0.3)
	160	(16.2 ± 0.3)

process temperatures above 140 °C only crystalline silver with a mean crystallite size ranging from 16 to 18 nm (Table 1) is detected (Fig. 5), indicating that also for sol *B* the crystallite size is not influenced by the processing temperature. While results from XRD measurements are in good accordance with the reduction of Ag^+ at increasing temperature, the interpretation of optical spectra from sol *A* and sol *B* is more challenging. Although sol *A* and sol *B* are prepared with the same amount of $AgNO_3$, these sols show different colorations and accordingly different optical spectra are observed. For sol *A* no single peak around a wavelength of 420 nm indicating the presence of nanosized crystalline silver [65–67] can be determined (Fig. 6). After conventional solvothermal processing at a temperature of 120 °C two peaks at 438 and 550 nm are observed, while with increasing temperature only one broad peak, whose intensity increases with reaction temperature, occurs. After

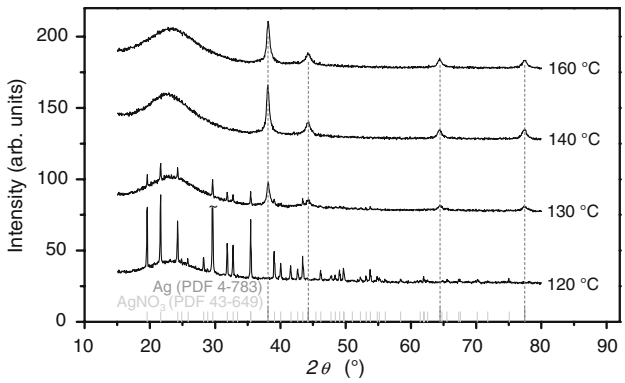

Fig. 5 XRD patterns of dried powders gained from sol *B* treated for 1 h in the conventional solvothermal process at different temperatures

microwave processing at a temperature of 120 °C sol *A* is almost transparent. This result is in good agreement with the high amount of Ag^+ in solution indicating that at a process temperature of 120 °C the reduction to silver particles does not yet occur. After microwave processing at a temperature of 130 °C analogously to the conventional process at a temperature of 120 °C a double peak in the optical spectra is observed. The peak maxima are at wavelength of 436 and 539 nm. Again, at higher processing temperatures only one broad absorption peak remains. From sol *B* a broad absorption, covering the whole visible range, is observed (Fig. 6), leading to the assumption that larger, probably polycrystalline, silver particles in a broad size distribution are present in the liquid. The presence of much larger silver particles in sol *B* could be the reason for the different coloration of sol *A* and sol *B* even though both sols contain the same silver concentration.

For a double peak structure of an optical spectrum of silver particles, several reasons are reported in literature, as e.g., particle aggregation [36, 68], electromagnetic coupling from cluster–cluster interaction [69] or an asymmetric particle shape (rod-like) [34, 70]. A red-shift of the absorption peak could be the result of particle interaction with the surrounding matrix [71], particle aggregation or simple formation of larger particles [36, 65]. In the HRTEM images of samples conventionally processed at a temperature of 120 °C (Fig. 7), the particles observed appear with different contrast and exhibit different shapes (round, triangular, hexagonal and rod-like). Analogous morphologies are found for the microwave processed sample prepared at 130 °C. In order to examine structural and morphological characteristics of the different particle species more in detail, HRTEM images with higher magnification are recorded (Fig. 8). As result of these investigations round particles, as well as particles with a distorted hexagonal-like morphology and blurry absorption contrast, can be identified as polycrystalline silver, while rod-like particles consist of a single silver crystallite. The triangular

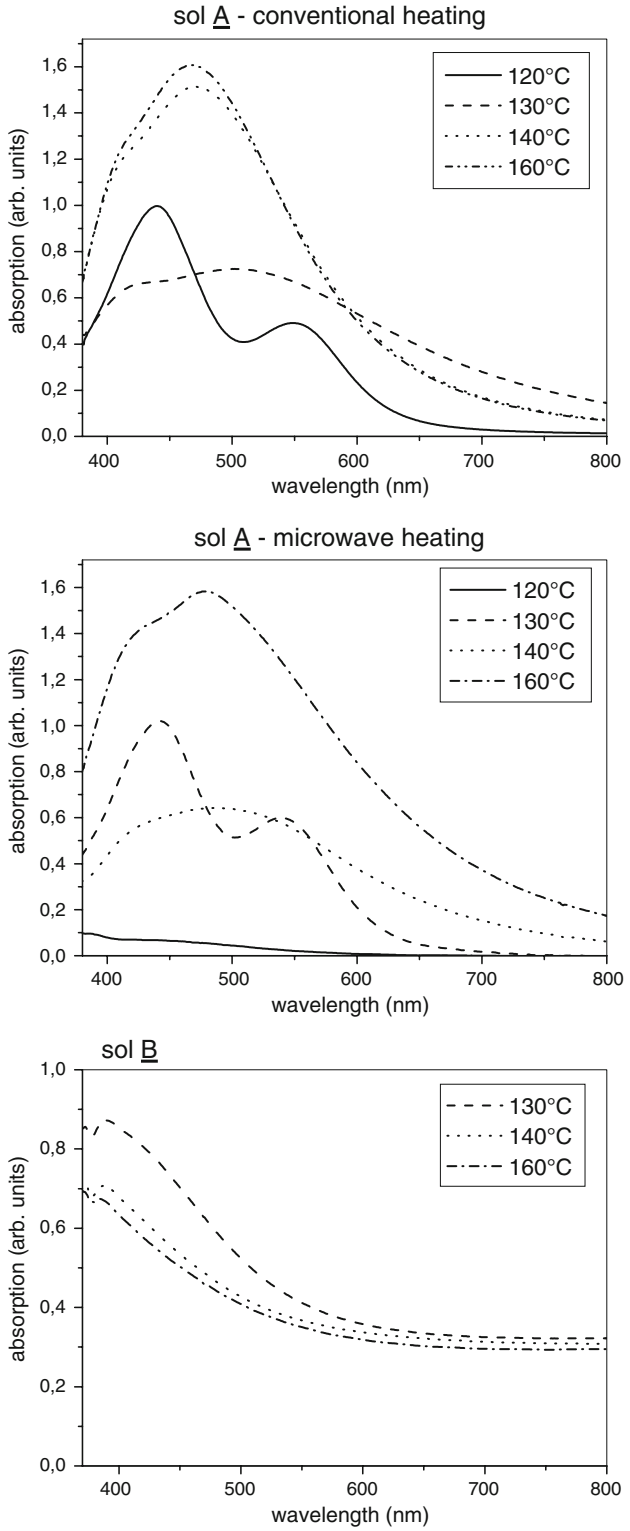

Fig. 6 Optical spectra of sol *A* and sol *B* prepared with different temperatures during the solvothermal process

and hexagonal particles, appearing with lower contrast compared to the round, distorted hexagonal and rod-like silver particles, can be identified as single crystalline $AgNO_3$ in its high-temperature rhombohedral phase (ICSD collection code N° 35157 [63]). It should be remembered here, that at the processing temperature of 120 °C almost 75% of not reduced $AgNO_3$ remains (compare Fig. 2). For this reason, the double peak structure in the optical spectrum could be attributed to the shape of the silver particles. At 140 °C the particle size increases simultaneously to the decrease of Ag^+ in solution but also the particle shape turns from more angular to round (Fig. 9).

Tsuji et al. [45] report the formation of triangular and rod-like morphologies for silver particles prepared in a polyol process in presence of PVP. It can be assumed that the polymer PVP plays a significant role by complexation of Ag^+ ions and controls the growth rate of the particles in certain crystallographic directions. More precisely it is reported that multiply twinned polycrystalline rod-like particles and wires with high aspect ratio growing in [111] direction develop due to long chain PVP complexation at (100) prism planes whereas single-crystalline triangular platelets evolve due to short chain PVP complexation at (111) faces and thus crystal growth in [100] direction. However, this polyol process only leads to these morphologies in presence of the nucleation agent H_2PtCl_6. Without nucleation agent, larger spherical silver particles are formed [45]. Other authors report different reduction conditions for $AgNO_3$ in presence of PVP leading to triangular and rod-like structures without the necessity of a noble metal nucleation agent [35, 36].

In comparison to the reports in literature above, after processing at a temperature of 120 °C different types of particles and particle morphologies are observed. Therefore, it could be concluded, that at first due to certain growth restriction resulting from the complexation with PVP different morphologies of silver particles are formed. The HRTEM image (Fig. 8b) shows that short rod-like particles develop extended (111) faces and are single crystalline. Thus, with respect to [45] the formation of this type of morphology is expected to be the result of PVP complexation at (111) faces and incipient growth in [100] direction. In further course of $AgNO_3$ reduction, the silver particles grow with a tendency to a more spherical morphology. Thus, the initial growth restrictions should be no longer valid when a certain particle size is exceeded. Accordingly, Wang et al. [72] report that silver particles with diameters smaller than 50 nm are protected by coordination between silver and N atoms in PVP. For larger particles a different coordination with both N atoms and O atoms is supposed. This leads to the assumption that in our study the different morphologies of particles up to 50 nm in diameter are the result of PVP coordination with N in a first stage of particle formation. If the particles grow larger than 50 nm in diameter, a different type of coordination by

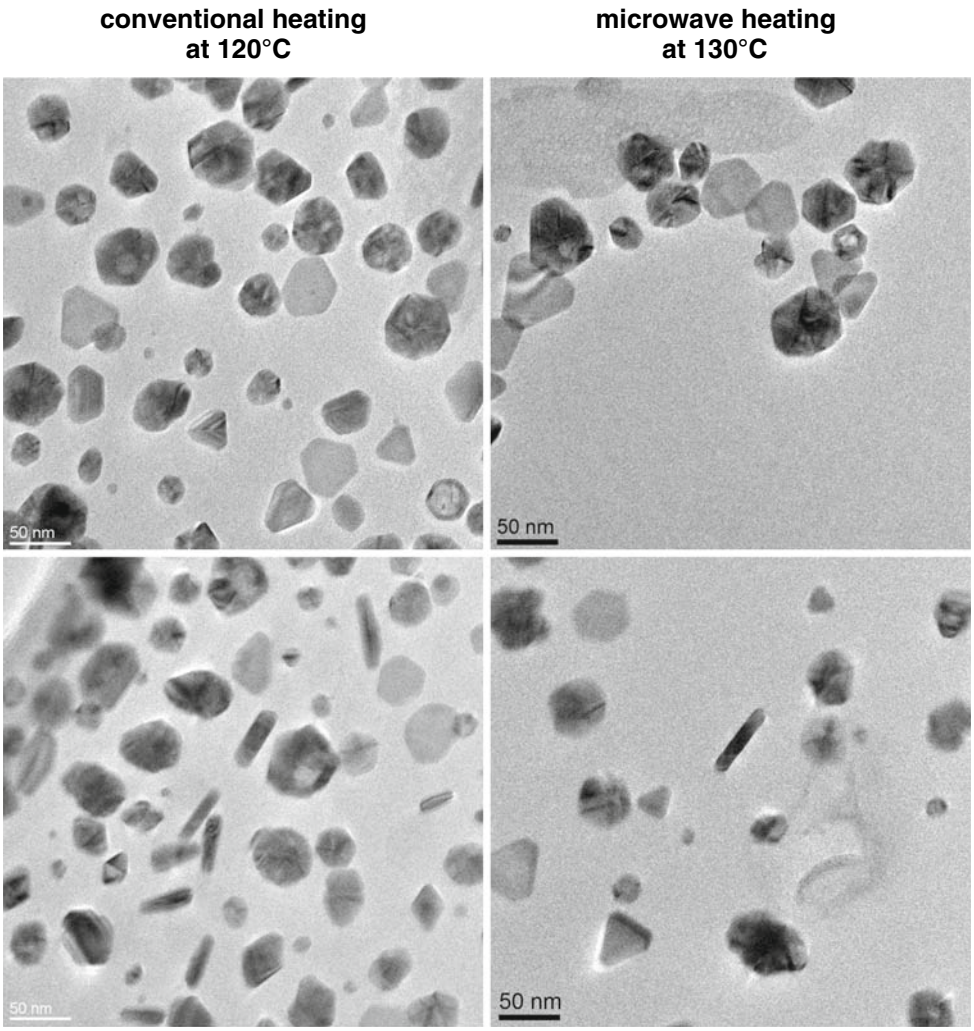

Fig. 7 HRTEM images of sol *A* after conventional solvothermal preparation at 120 °C and microwave solvothermal preparation at 130 °C. From every sample two different images are presented

PVP occurs leading to a more spherical morphology. The HRTEM images as well as the analogous optical spectra do not show significant differences in particle morphology in sols obtained by conventional thermal and microwave processing. Samples prepared at lower temperature, generating the double peak in the optical spectra, exhibit different types of silver particle morphologies as rod-like, spherical and distorted hexagonal. Samples prepared at a higher processing temperature of 140 °C exhibit for both heating procedures larger and less angular particles. With microwave processing the particles prepared at 140 °C are around three times larger than the conventionally prepared ones (Fig. 9). Therefore, it should be concluded that for the synthesis of silver nanoparticles presented here, mainly the process temperature and time duration have an influence on the particle morphology. The larger particle size of microwave processed sols at a temperature of 140 °C compared to conventional thermal preparation may be explained by strong interactions of the silver particles with microwaves leading to a locally higher temperature which enhances the particle growth [55]. In literature it is often reported that for microwave-assisted synthesis of nanoparticles different particle morphologies are observed in comparison to conventional thermal preparation [73–75], e.g., rice grain structures for $SrWO_4$ in solvothermal preparation under microwave radiation [73]. However, for the synthesis of silver nanoparticles in presence of PVP studied here, the difference in particle morphology, resulting from different heating procedures (conventional thermal or microwave-assisted) seems to be only marginally.

The change of particle size with solvothermal temperature, estimated from optical spectra and HRTEM is also determined by particle size distribution by DLS in solution (Fig. 10). For the reaction temperature of 120 °C, the particle size distribution of sol *A* has a maximum at 27 nm while at 140 °C prepared sol shows the maximum is at 131 nm. For sol *B* the broad optical spectra correspond to a broad particle size distribution with a maximum at 70 nm for reaction temperature of 130 °C and a distribution over

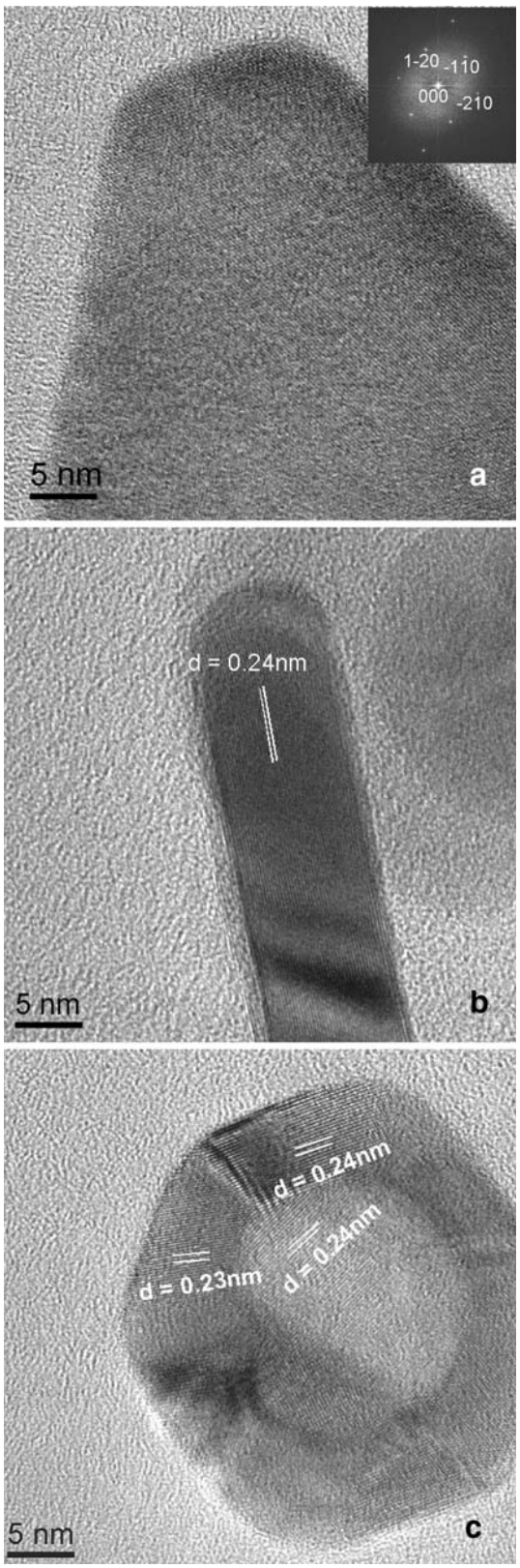

◀ **Fig. 8** HRTEM images of different particle species of sol *A* after conventional solvothermal preparation at 120 °C. Triangular single crystalline $AgNO_3$ particle (**a**), rod-like single-crystalline silver particle (**b**) and spherical polycrystalline silver particle (**c**). The inset in (**a**) shows the Fast Fourier Transformation of the image area. Reflections indicated correspond to $AgNO_3$ (ICSD collection code N° 35157 [63]). In (**b**) and (**c**) measured *d*-spacings of Ag (111) lattice planes identified (theoretical value $d = 0.2359$ nm, according to ICSD collection code N° 64706 [61]) are given

several hundred nanometers for sols prepared at 140 and 160 °C (Fig. 10). According to XRD evaluations, these samples contain silver crystallites of diameters smaller than 20 nm, so it can be stated, that the much larger particles determined by DLS are polycrystalline. Since the crystallite size does not increase with processing temperature, an increasing particle size can be determined with increasing temperature. It can be stated that with higher temperatures larger polycrystalline particles are formed, while the size of the crystallite phases remains unchanged. Furthermore, sol *B* prepared at 140 °C precipitates in 1 week, however, the redispersion is easily possible. Therefore, it seems that the presence of SiO_2 could disturb the stabilisation of small silver particles by PVP, so at high reaction temperatures there is no limitation of particle growth and the silver particles are less stable in solution. This behavior is different to that of silver particles prepared in presence of ethanolamines, as reported earlier [76]. In that case the limitation of growth of silver particles can be induced by the presence of nanoscale SiO_2 particles. It seems that the polymeric surfactant PVP is a better stabilizer for the formed Ag particles than the reported ethanolamines, so in presence of PVP additional SiO_2 particles are not necessary for stabilisation of silver particles.

3.3 Antimicrobial properties

The solutions containing crystalline silver are applied onto textile materials to test their antimicrobial properties. As expected, coated textile samples show a high antimicrobial effect against the bacteria *E.coli.* In case of household washing the antimicrobial effect is decreased but still present (Fig. 11). The washing fastness decreases with higher process temperature indicating that larger silver particles are probably less adhesive on textile fibers. With sol *B* prepared at 130 °C the best wash stability is reached, indicating that the presence of SiO_2 particles causes a certain improvement of adhesion due to film formation. However, even with sol *A* containing no SiO_2, a significant antimicrobial effect can be determined after washing. This fact could be explained by adhesive forces between the silver nanoparticles and functional groups on the fiber surface, most probably the OH-groups of the viscose fabric. The silver nanoparticles are elemental and in contrast to $AgNO_3$ not soluble in aqueous washing solutions, so the washing stability should be mainly governed by the adhesion of these silver particles to the textile fiber.

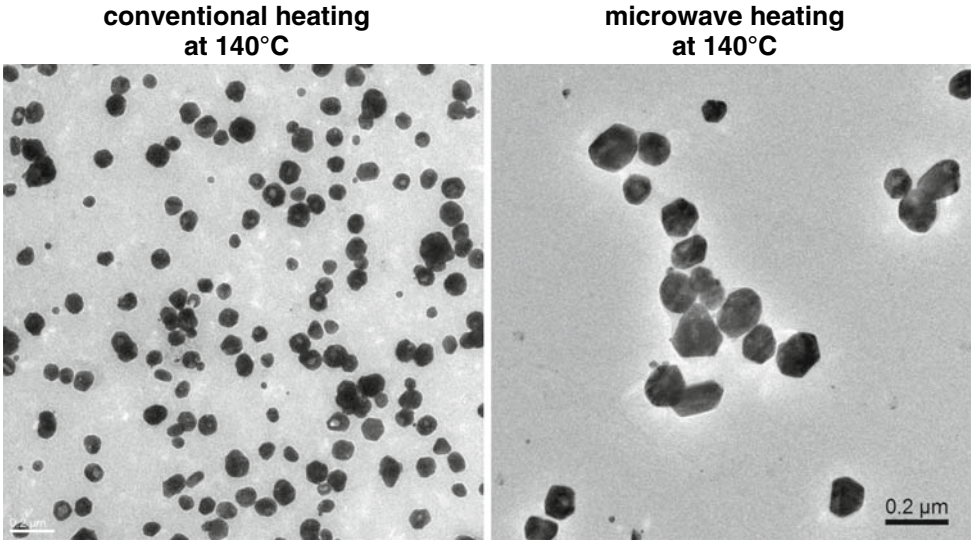

Fig. 9 HRTEM image of sol *A* after conventional and microwave solvothermal preparation at 140 °C

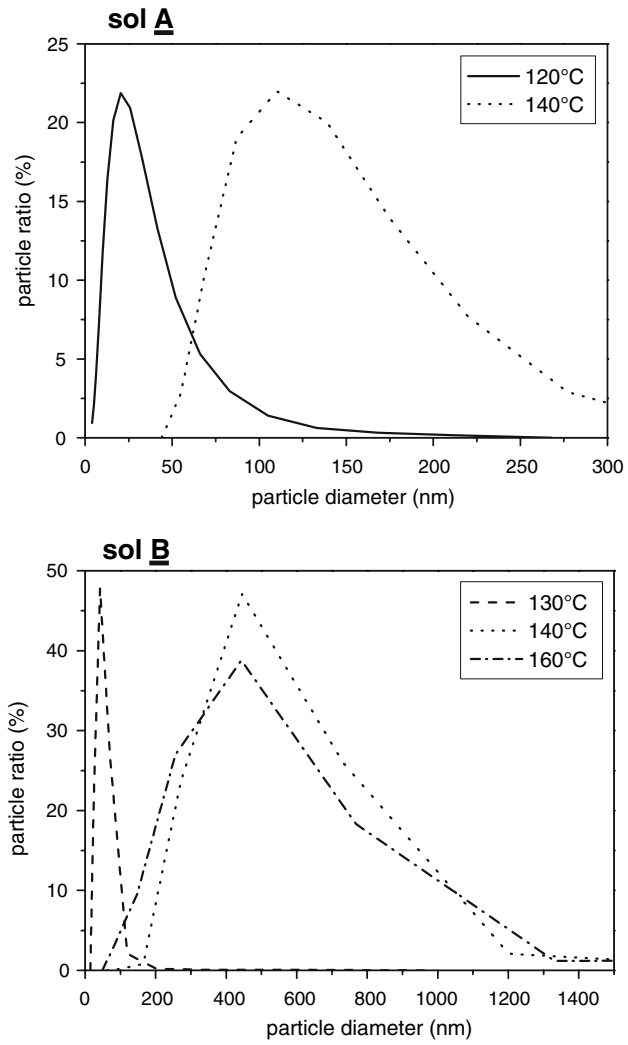

Fig. 10 Particle size distribution in solution (by DLS) after conventional solvothermal preparation at different temperatures

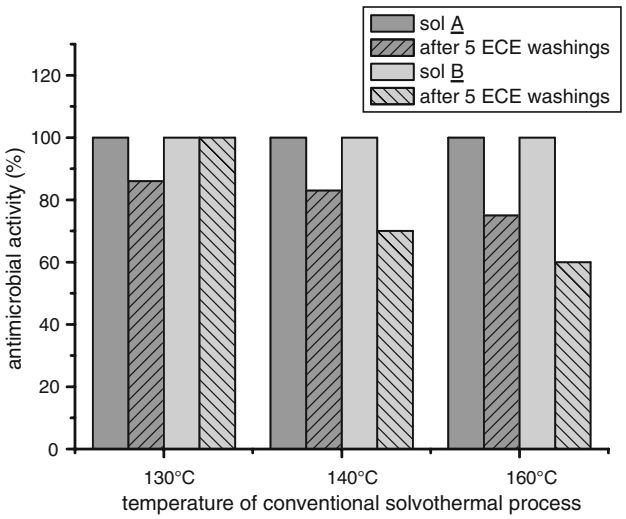

Fig. 11 Antimicrobial activity against *E. coli* on coated viscose fabrics after coating preparation and after five times repeated household washing procedure

4 Conclusions

The preparation of coating solutions of silver nanoparticles and Ag/SiO_2 composites can be achieved by using a solvothermal process with conventional and microwave heating. No significant difference in particle morphology is observed for the different heating procedures. For preparation of crystalline silver nanoparticles temperatures of at least 120 °C are necessary in this solvothermal process. In the temperature range between 120 and 130 °C the formation rate of silver nanoparticles is very sensitive to temperature variations and processing time. Furthermore, in this temperature range several different morphologies of

silver nanoparticles are observed, as rod-like, spherical or distorted hexagonal shapes, which are probably the result of complexing the growing particle with the polymer PVP. However, higher processing temperatures lead to more uniform, less angular and larger polycrystalline silver particles. The coating solutions can be easily applied onto textiles by dip-coating. The antimicrobial properties of the textile fabrics treated, are even present after several times of washing under household conditions.

Acknowledgments For financial support we owe many thanks to the German Bundesministerium für Wirtschaft und Technologie within the framework of the research program "Industrielle Vorlaufforschung"—project number: VF070012. We would like to thank Dr. H. Staufenberg, CEM GmbH, who enables the experiments with the microwave autoclave Discover Labmate™.

References

1. Lee HJ, Yeo SY, Jeong SH (2003) J Mater Sci 38:2199. doi:10.1023/A:1023736416361
2. Stobie N, Duffy B, McCormack DE, Colreavy J, Hidalgo M, McHale P, Hinder SJ (2008) Biomaterials 29:963. doi:10.1016/j.biomaterials.2007.10.057
3. Albrecht-Mackenneth K (2003) German Patent DE10137477
4. Schneider S, Halbig P, Grau H, Nickel U (1994) Photochem Photobiol 60:605. doi:10.1111/j.1751-1097.1994.tb05156.x
5. Carotenuto G, Pepe GP, Nicolais L (2000) Eur Phys J B 16:11. doi:10.1007/s100510070243
6. Lee HJ, Jeong SH (2004) Text Res J 74:442. doi:10.1177/004051750407400511
7. Yuranova T, Rincon AG, Pulgarin C, Laub D, Xantopoulos N, Mathieu H-J, Kiwi J (2006) J Photochem Photobiol Chem 181:363. doi:10.1016/j.jphotochem.2005.12.020
8. Haug S, Roll A, Schmid-Grendelmeier P, Johansen P, Wütherich B, Kündig TM, Senti G (2006) Curr Probl Dermatol 33:144. doi:10.1159/000093941
9. Mahltig B, Haufe H, Böttcher H (2005) J Mater Chem 15:4385. doi:10.1039/b505177k
10. Mahltig B, Textor T (2008) Nanosols and Textiles. World Scientific, Singapore
11. Mahltig B, Swaboda C, Roessler A, Böttcher H (2008) J Mater Chem 18:3180. doi:10.1039/b718903f
12. Haufe H, Muschter K, Siegert J, Böttcher H (2008) J Sol-Gel Sci Technol 45:97. doi:10.1007/s10971-007-1636-5
13. Xing Y, Yang X, Dai J (2007) J Sol-Gel Sci Technol 43:187. doi:10.1007/s10971-007-1575-1
14. Fir M, Vince J, Vuk AS, Vilcnik A, Jovanovski V, Mali G, Orel B, Simomcic B (2007) Acta Chim Slov 54:144
15. Li FY, Xing YJ, Ding X (2007) Enzyme Microb Technol 40:1692. doi:10.1016/j.enzmictec.2006.09.007
16. Abidi N, Hequet E, Tarimala S, Dai LL (2007) J Appl Polym Sci 104:111. doi:10.1002/app.24572
17. Nedelcev T, Krupa I, Lath D, Spírková M (2008) J Sol-Gel Sci Technol 46:47. doi:10.1007/s10971-008-1713-4
18. Tomsic B, Simoncic B, Orel B, Cerne L, Forte Tavcer P, Zorko M, Jerman I, Vilcnik A, Kovac J (2008) J Sol-Gel Sci Technol 47:44. doi:10.1007/s10971-008-1732-1
19. Mennig M, Schmitt M, Schmidt H (1997) J Sol-Gel Sci Technol 8:1035
20. Armelao L, Bertoncello R, De Dominicis M (1997) Adv Mater 9:736. doi:10.1002/adma.19970090913
21. Kawashita M, Tsuneyama S, Miyaji F, Kokubo T, Kozuka H, Yamamoto K (2000) Biomaterials 21:393. doi:10.1016/S0142-9612(99)00201-X
22. Mahltig B, Fiedler D, Böttcher H (2004) J Sol-Gel Sci Technol 32:219. doi:10.1007/s10971-004-5791-7
23. Kovalenko DL, Gurin VS, Bogdanchikova NE, Prokopenko VB, Alexxeenko AA, Melnichenko IM (2002) J Alloy Comp 341:208. doi:10.1016/S0925-8388(02)00078-6
24. Ritzner B, Villegas MA, Fernández Navarro JM (1997) J Sol-Gel Sci Technol 8:917
25. Mahltig B, Gutmann E, Meyer DC, Reibold M, Dresler B, Günther K, Faßler D, Böttcher H (2007) J Mater Chem 17:2367. doi:10.1039/b702519j
26. De G, Licciulli A, Massaro C, Tapfer L, Catalano M, Battaglin G, Meneghini C, Mazzoldi P (1996) J Non-Cryst Solids 194:225. doi:10.1016/0022-3093(91)00511-F
27. Weiping C, Lide Z (1997) J Phys Condens Matter 9:7257. doi:10.1088/0953-8984/9/34/015
28. Chakrabarti K, Whang CM (2002) Mater Sci Eng B 88:26. doi:10.1016/S0921-5107(01)00908-4
29. Wu P-W, Dunn B, Doan V, Schwartz BJ, Yablonovitch E, Yamane M (2000) J Sol-Gel Sci Technol 19:249. doi:10.1023/A:1008748608055
30. Ritzer B, Villegas MA, Fernández Navarro JM (1995) Glastechn Ber Glass Sci Technol 68(C1):417
31. Martínez-Castanón G, Martínez JR, Ortega Zarzosa G, Ruiz F, Sánchez-Loredo MG (2005) J Sol-Gel Sci Technol 36:137. doi:10.1007/s10971-005-5285-2
32. Guzmán MG, Dille J, Godet S (2008) Proceedings of World Academy of Science. Eng Technol 33:367
33. Zhang Z, Zhao B, Hu L (1996) J Solid State Chem 121:105. doi:10.1006/jssc.1996.0015
34. Chou K-S, Ren C-Y (2000) Mater Chem Phys 64:241. doi:10.1016/S0254-0584(00)00223-6
35. Chou K-S, Lai Y-S (2004) Mater Chem Phys 83:82. doi:10.1016/j.matchemphys.2003.09.026
36. Deivaraj TC, Lala NL, Lee JY (2005) J Colloid Interface Sci 289:402. doi:10.1016/j.jcis.2005.03.076
37. Chou K-S, Chen C-C (2007) Microporous Mesoporous Mater 98:208. doi:10.1016/j.micromeso.2006.09.006
38. Slistan-Grijalva A, Herrera-Urbina R, Rivas-Silva JF, Ávalos-Borja M, Castillón-Barraza FF, Posada-Amarillas A (2008) Mater Res Bull 43:90. doi:10.1016/j.materresbull.2007.02.013
39. Hirai H, Nakao Y, Toshima N (1979) J Macromol Sci-Chem A13:727. doi:10.1080/00222337908056685
40. Wang H, Qiao X, Chen J, Wang X, Ding S (2005) Mater Chem Phys 94:449. doi:10.1016/j.matchemphys.2005.05.005
41. Silvert P-Y, Herrera-Urbina R, Duvauchelle N, Vijayakrishman V, Elhsissen KT (1996) J Mater Chem 6:573. doi:10.1039/jm9960600573
42. Ducamp-Sanguesa C, Herrera-Urbina R, Figlarz M (1992) J Solid State Chem 100:272. doi:10.1016/0022-4596(92)90101-Z
43. Liu X, Zhang F, Huang R, Pan C, Zhu J (2008) Cryst Growth Des 8:1916. doi:10.1021/cg701128b
44. Chen D, Gao L (2004) J Cryst Growth 264:216. doi:10.1016/j.jcrysgro.2003.12.019
45. Tsuji M, Nishizawa Y, Matsumoto K, Kubokawa M, Miyamae N, Tsuji T (2006) Mater Lett 60:834. doi:10.1016/j.matlet.2005.10.027
46. Hah HJ, Koo SM, Lee SH (2003) J Sol-Gel Sci Technol 26:467. doi:10.1023/A:1020710307359
47. Goia DV, Matijevic E (1998) N J Chem 11:1203. doi:10.1039/a709236i
48. Wie G, Nan C-W, Deng Y, Lin Y-H (2003) Chem Mater 15:4436. doi:10.1021/cm034628v
49. Gao F, Lu Q, Komarneni S (2005) Chem Mater 17:856. doi:10.1021/cm048663t

50. Zhang YC, Wang GY, Hu XY, Xing R (2005) J Solid State Chem 178:1609. doi:10.1016/j.jssc.2005.03.009
51. Grocholl L, Wang J, Gillan EG (2003) Mater Res Bull 38:213. doi:10.1016/S0025-5408(02)01028-0
52. Yang Y, Matsubara S, Xiong L, Hayakawa T, Nogami M (2007) J Phys Chem C 111:9095. doi:10.1021/jp068859b
53. Tian C, Mao B, Wang E, Kang Z, Song Y, Wang C, Li S, Xu L (2007) Nanotechnology 18:285607. doi:10.1088/0957-4484/18/28/285607
54. Vigneshwaran N, Kate AA, Varadarajan PV, Nachane RP, Balasubramanya RH (2007) J Nanosci Nanotechnol 7:1. doi:10.1166/jnn.2007.737
55. Rao KJ, Vaidhyanathan B, Ganguli M, Ramakrishnan PA (1999) Chem Mater 11:882. doi:10.1021/cm9803859
56. Marques VS, Cavalcante LS, Sczancoski JC, Volanti DP, Espinosa JWM, Joya MR, Santos MRMC, Pizani PS, Varela JA, Longo E (2008) Solid State Sci 10:1056. doi:10.1016/j.solidstatesciences.2007.11.004
57. Powder Diffraction File 2, release 2001 (2001) Joint Committee on Powder Diffraction Standards–International Centre for Diffraction Data (JCPDS–ICDD)
58. TOPAS (2000) General Profile and Structure Analysis Software for Powder Diffraction Data, V2.0, Bruker AXS GmbH, Karlsruhe, Germany
59. Cheary RW, Coelho AA (1992) J Appl Cryst 25:109. doi:10.1107/S0021889891010804
60. Inorganic Crystal Structure Database (ICSD) (2008) FINDIT, V1.1.4, FIZ Karlsruhe, Germany
61. Swenson HE, Tatge E (1953) National Bureau of Standards (U.S.). Circular 539:1
62. Berar JF, Lelau P (1991) J Appl Cryst 24:1. doi:10.1107/S0021889890008391
63. Meyer P, Capponi JJ (1982) Acta Crystallogr B 38:2543. doi:10.1107/S0567740882009352
64. Zhang WC, Wu XL, Chen HT, Gao YJ, Zhu J, Huang GS, Chu PK (2008) Acta Mater 56:2508. doi:10.1016/j.actamat.2008.01.043
65. Kreibig U, Vollmer M (1995) Optical properties of metal clusters. Springer, Heidelberg
66. Creighton JA, Eadon DG (1991) J Chem Soc, Faraday Trans 87:3881. doi:10.1039/ft9918703881
67. Salz D, Lamber R, Wark M, Baalmann A, Jaeger N (1999) Phys Chem Chem Phys 1:4447. doi:10.1039/a904175c
68. Berger A, Berg K-J, Hofmeister H (1991) Z Phys D 20:309. doi:10.1007/BF01543998
69. Salz D, Wark M, Baalmann A, Simon U, Jaeger N (2002) Phys Chem Chem Phys 4:2438. doi:10.1039/b111038a
70. Yu YY, Chang SS, Lee CL, Wang CRC (1997) J Phys Chem 101:6661. doi:10.1021/jp971656q
71. Hövel H, Fritz S, Hilger A, Kreibig U, Vollmer M (1993) Phys Rev B 48:18178. doi:10.1103/PhysRevB.48.18178
72. Wang H, Qiao X, Chen J, Wang X, Ding S (2005) Mater Chem Phys 94:449. doi:10.1016/j.matchemphys.2005.05.005
73. Sczancoski JC, Cavalcante LS, Joya MR, Espinosa JWM, Pizani PS, Varela JA, Longo E (2009) J Colloid Interface Sci 330:227. doi:10.1016/j.jcis.2008.10.034
74. Thongtem T, Phuruangrat A, Thongtem S (2008) Curr Appl Phys 8:189. doi:10.1016/j.cap.2007.08.002
75. Thongtem T, Phuruangrat A, Thongtem S (2008) Mater Lett 62:454. doi:10.1016/j.matlet.2007.05.059
76. Mahltig B, Gutmann E, Meyer DC, Reibold M, Bund A, Böttcher H (2009) J Sol-Gel Sci Technol 49:202. doi:10.1007/s10971-008-1836-7